The Hermite Transform: An Alternative Image Representation Model for Iris Recognition

Alfonso Estudillo-Romero and Boris Escalante-Ramirez

Universidad Nacional Autonoma de Mexico, Fac. de Ingenieria, Edif. de Posgrado e Investigacion, Ciudad Universitaria, C.P. 04510, Mexico, D.F., Mexico
aestudillor@uxmcc2.iimas.unam.mx,
boris@servidor.unam.mx

Abstract. In this work we propose an alternative image representation model to efficiently characterize iris textures based on the Hermite transform. The Hermite transform can simulate some properties of the mammalian visual system and it is founded on a well established mathematical framework. These properties are used to extract the most important information of the iris textures. The results show that the Hermite transform is able to characterize iris textures as well as the Gabor model, with the advantage on the second that the discrete analysis filters in the Hermite transform are given by the Krawtchouk polynomials and, it is not needed to compute the filter coefficients by means of optimization methods, nor to suppress the zero mean (d.c. response). The proposed iris recognition system achieved an overall performance of 97.34% and a Correct Access Rate (CAR) of 90.29% when the False Access Rate (FAR) was closed to zero.

Keywords: Biometrics, Iris Recognition, Hermite Transform.

1 Introduction

Nowadays, efficient methods for confident recognition of persons on a wide range of applications are needed. To accomplish such tasks, different biometric technologies have emerged, e.g. fingerprint, face and iris recognition systems. Iris recognition has shown to be one of the most accurate biometric systems when a high level of security is required.

A typical iris recognition system is composed of three major stages: acquisition, feature extraction and matching. In the first stage, the iris images are acquired with a camera, and this is frequently done under controlled conditions, such as near infrared (NIR) illumination [1]. The feature extraction stage involves two preprocessing tasks: a) the region of interest (ROI) on the input image, i.e., the iris, must be localized and b) depending on the implemented system, the iris images are normalized in order to have the same size. The most important features of the iris are extracted through an image representation model and then encoded on a biometric template. During the last stage, the biometric templates are matched and, depending on the distance criteria selected, the system accepts or rejects a claimed identity either for authentication or for identification.

J. Ruiz-Shulcloper and W.G. Kropatsch (Eds.): CIARP 2008, LNCS 5197, pp. 86–93, 2008.

Different image representation models for the iris texture feature extraction have been previously reported, e.g. Gabor wavelets [1], Haar wavelet [2] and Daubechies wavelet [3]. Image representation models inspired on biological visual systems are of special interest, because they take advantage of some properties at cortical levels and use them to extract visual information from images in the same way that such systems do.

The fact that Gabor wavelets are able to fit the receptive field profiles (RFP) of simple cells in the primary visual cortex and the optimal conjoint resolution of information in the 2D spatial and 2D Fourier domains that can be achieved [4], have made them widely used to extract local features in many applications related to texture characterization. However, the selection of the filter coefficients is not obvious and this is often done by sampling the continuous Gabor function [5] or by optimization methods (see [6] for some filter selection methods).

The Hermite transform, firstly introduced to the digital image processing area by Martens [7], is a local decomposition technique in which an input image is localized through a Gaussian window and projected over orthogonal basis with respect to such window. The connection between the Hermite transform and mammalian visual systems comes from the fact that the elementary functions used in the Hermite transform are similar to the Gaussian derivatives. Young [8] discovered the match in shape between the Gaussian derivatives functions and the RFP of primate simple cells.

We present the Hermite transform as an alternative image representation model for feature extraction applied to iris texture characterization. The Hermite transform has been previously used for local orientation analysis [9] and a Gabor-like Hermite model has been used for texture indexing [10]. In Sect. 2 the Hermite transform and the discrete Hermite analysis functions are presented. Section 3 describes the stages involved in the proposed iris recognition system. Results with the Hermite transform as an iris texture feature extractor are reported in Sect. 4. Finally, conclusions and future works are given in Sect. 5.

2 The Hermite Transform

The Hermite transform is a local decomposition technique, in which an input signal $L(x)$ is localized through a Gaussian window $V(x)$ and then expanded into orthogonal Hermite polynomials $H_n\left(\frac{x}{\sigma}\right)$ at every window position [7]. The expansion coefficients $L_n(x)$ can be derived by convolution of the signal with the Hermite analysis functions.

2.1 Hermite Analysis Functions

The one dimensional analysis functions of the Hermite transform of degree n are defined as follows [7]:

$$D_n(x) = \frac{(-1)^n}{\sqrt{2^n n!}} \cdot \frac{1}{\sigma\sqrt{\pi}} H_n\left(\frac{x}{\sigma}\right) e^{-\frac{x^2}{\sigma^2}} \quad . \tag{1}$$

where σ is the standard deviation of the Gaussian window. $H_n(x)$ are the Hermite polynomials given by Rodrigues' formula:

$$H_n(x) = (-1)^n e^{x^2} \frac{d^n e^{-x^2}}{dx^n}, \quad n = 0, 1, 2, \dots \ . \tag{2}$$

The two dimensional analysis functions have the advantage to be separable and they can be written as:

$$D_{n-m,m}(x, y) = D_{n-m}(x) D_m(y) \ . \tag{3}$$

where $n - m$ and m denote the analysis order in x and y direction respectively. We then can expand a given input image $L(x, y)$ into the basis $D_{n-m,m}(x, y)$ as:

$$L_{n-m,m}(x_0, y_0) = \int_x \int_y L(x, y) D_{n-m,m}(x_0 - x, y_0 - y) dx dy \ . \tag{4}$$

for $n = 0, 1, \dots, d_{max}$ and $m = 0, \dots, n$, where d_{max} is the maximum desired derivative degree.

2.2 Discrete Hermite Analysis Functions

The discrete equivalent form of the analysis functions are the Krawtchouk filters. These are defined as Krawtchouk polynomials multiplied by a binomial window $v^2(x) = C_N^x / 2^N$. The binomial window approximates the discrete Gaussian window, and is given by:

$$C_N^x = \frac{N!}{x!(N - x)!} \ . \tag{5}$$

where N is the length of the binomial window. Then, the orthonormal Krawtchouk polynomials can be written as follows:

$$K_n(x) = \frac{1}{\sqrt{C_N^n}} \sum_{\tau=0}^{n} (-1)^{n-\tau} C_{N-x}^{n-\tau} C_x^\tau \ . \tag{6}$$

for $x = 0, ..., N$ and $n = 0, ..., d_{max}$, with $d_{max} \leq N$. The discrete Hermite transform of length N approximates the continuous form of the Hermite transform with $\sigma = \sqrt{N/2}$ [7].

3 Proposed Iris Recognition System

A typical iris recognition system can be divided in three major stages as shown in Fig. 1. In order to test our proposed feature extractor, we have developed an iris recognition system based on these stages [1].

Fig. 1. Typical iris recognition stages

3.1 Acquisition

An iris recognition system must be able to capture the iris texture information regardless of colour and size of the iris. It has been suggested the use of monochrome cameras and NIR illumination to avoid specular reflections [1]. We have tested our feature extractor using the CASIAv1.0 iris image database [11], whose images have been captured under such conditions. It comprises 756 iris images from 108 different persons. We have used the second set, in which 4 images belong to the same eye comprising a total of 432 images. Each grayscale iris image has a resolution of 320×280 pixels.

3.2 Preprocessing

Before the feature extraction begins, the iris must be localized into the image. The circular Hough transform was adopted to approximate the pupil and iris boundaries as two non-concentric circles [1]. In order to apply the Hough transform, a binary edge map must be generated. The Canny edge detector [12] was used to accomplish such task.

Following [13], the gradient orientation on the circumference of a circle is pointing towards its centre. This property is used to find the center coordinates of the two circles with one 2D accumulator for each one, $C_p[x, y]$ for the pupil and $C_i[x, y]$ for the iris. Possible centers can be approximated by taking the intersections from every binary edge projection along its gradient orientation between a minimum and maximum radius ($r_{min} \leq r \leq r_{max}$). A given projection intersecting another one represents a vote for the possible center coordinates, which is stored on the accumulator in such coordinates by increasing its value one unit. Circle centers are then determined by choosing the most voted coordinates from each one of the two accumulators $C_p[x, y]$ and $C_i[x, y]$. Figure 2(a) shows the C_p accumulator over the input image after voting for possible pupil centers.

The pupil and iris radii are determined in a similar way. 1D accumulators were used to store votes for possible radii, $R_p[r]$ accumulates votes for the pupil radius and $R_i[r]$ for the iris radius. From each circle center, a search of edges belonging to the binary edge map between a minimum and maximum radius ($r_{min} \leq r \leq r_{max}$) is made. The radii are selected from each of the two accumulators by taking the most voted ones. Figure 2(b) and Fig. 2(c) show the pupil and iris radii searching procedure.

The search for the parameters of both pupil and iris was restricted to edges whose gradient orientation was into the intervals $[-2\pi/5, 2\pi/5]$, $[4\pi/5, \pi]$ and $[-4\pi/5, -\pi]$ for the pupil localization and $[-\pi/4, \pi/4]$, $[3\pi/4, \pi]$ and $[-3\pi/4, -\pi]$ for the iris localization, because of eyelids and eyelashes obstructions.

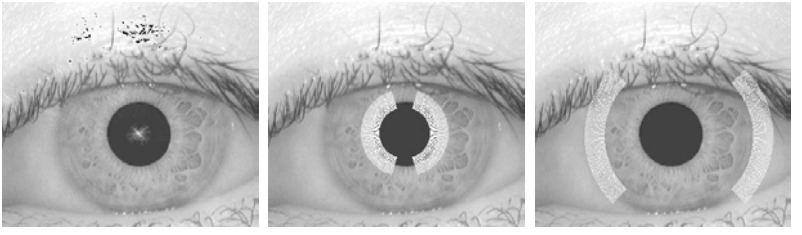

(a) (b) (c)

Fig. 2. Hough transform: pupil center (a), pupil (b) and iris (c) radii parameterization

In order to have images of the same size, a normalization procedure is made over the localized iris, which involves the use of pseudo-polar coordinates [1]:

$$I(x(r,\theta), y(r,\theta)) \rightarrow I(r,\theta) \ . \tag{7}$$

where $r \in [0,1]$ is the normalized distance taken for each $\theta \in [0, 2\pi]$ as a lineal combination of the pupil $(x_p(\theta), y_p(\theta))$ and iris $(x_i(\theta), y_i(\theta))$ elements, which are defined as:

$$x(r,\theta) = (1-r)x_p(\theta) + rx_i(\theta) \ . \tag{8}$$

$$y(r,\theta) = (1-r)y_p(\theta) + ry_i(\theta) \ . \tag{9}$$

Figure 3(a) shows the normalized iris image. In many cases, the eyelids and eyelashes appear after normalization as ellipses. They were approximated with an elliptic Hough transform and then suppressed (Fig. 3(b)). A mask of zeros and ones is also created. When an artefact is detected in a given position, the mask in such position is set to zero.

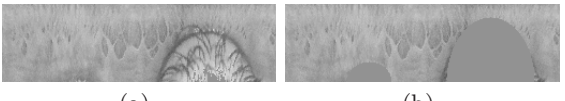

(a) (b)

Fig. 3. (a) Normalization of the ROI. (b) Suppression of eyelids and eyelashes.

3.3 Feature Extraction

Since the iris texture patterns tend to extend radially across the iris, the most important visual information is extracted from the normalized iris image by convolution with a pair of even (Fig. 4(a)) and odd (Fig. 4(b)) Hermite analysis filters, which can be formed by combining the Hermite analysis functions of second and first orders [14]. The outputs are then encoded in a similar way as [1]:

$$L_{2,0}(x_0, y_0) = \ \text{sgn} \int_x \int_y L(x,y) D_{2,0}(x_0 - x, y_0 - y) dxdy \ . \tag{10}$$

$$L_{1,0}(x_0, y_0) = \ \text{sgn} \int_x \int_y L(x,y) D_{1,0}(x_0 - x, y_0 - y) dxdy \ . \tag{11}$$

where $L_{2,0}$ and $L_{1,0}$ are either 1 or 0 depending on the sign of the 2D integral.

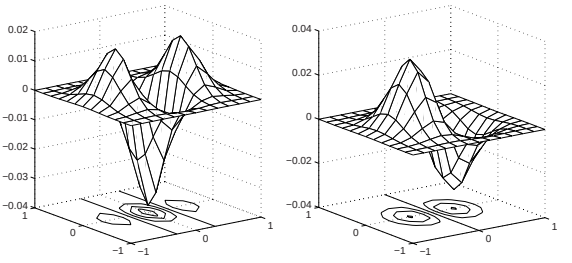

(a) (b)

Fig. 4. Proposed feature extractor: pair of even (a) and odd (b) Hermite analysis filters

3.4 Matching

The dissimilarity between biometric iris templates ($\bigotimes$ operator) is measured using the normalized Hamming distance (HD) criteria. The HD gives the number of bits that differ between two biometric iris templates of size N. The $\cap$ operator avoids to take into account eyelids and eyelashes obstructions in every biometric template comparison:

$$\mathrm{HD} = \frac{\sum_{j=1}^{N} (TempA_j \bigotimes TempB_j) \cap maskA_j \cap maskB_j}{\sum_{i=1}^{N} maskA_i \cap maskB_i} \quad . \tag{12}$$

4 Experimental Results

Experiments were conducted in order to evaluate the ability of the Hermite transform to characterize iris textures. As mentioned earlier, the CASIAv1.0 [11] iris image database was used. A total of 412 intra-class and 2628 inter-class comparisons were made between biometric iris templates of 2048 bits. Figure 5(a) shows such distributions. The media and standard deviation for the intra-class comparisons were $\mu_1 = 0.3146$ and $\sigma_1 = 0.0490$. For the inter-class comparisons the media was $\mu_2 = 0.4421$ whereas the standard deviation was $\sigma_2 = 0.0187$.

The overall system achieved an Equal Error Rate (EER) of 2.66%, Fig. 5(b). There is a compromise in every recognition system between correct rejections and false accesses to impostors. Ideal recognition systems should accept every registered user and reject all the impostors. To evaluate such requirement on the proposed iris recognition system, the False Access Rate (FAR) was set to zero and, then no impostor was able to access the system. With this constraint the False Rejection Rate (FRR) was 9.71%, which means that from the whole number of trials, when registered users try to be recognized, 90.29% are given correctly access to the system (CAR).

As can be seen on Table 1, results using the Daubechies 2 wavelet [3] show lower FRR, however the authors use only the lower half of the iris, having less probability to take into account artefacts due to inaccurate localization. Daugman [15] reports higher performance using the Gabor wavelet, but no fair comparisons can be made because access to the reported database is restricted.

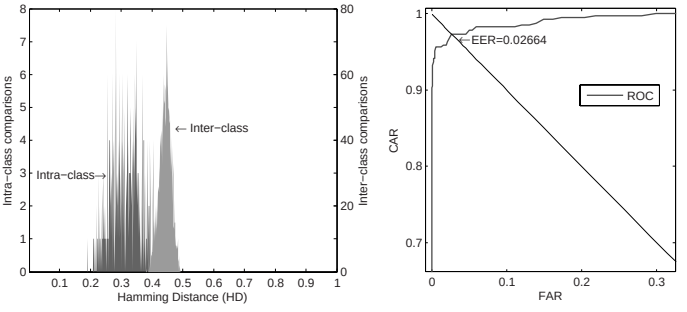

(a) (b)

Fig. 5. (a) Distributions of intra-class and inter-class comparisons. (b) Performance of the Hermite feature extractor (zoom of the ROC curve for visualization purposes).

Table 1. Comparison with other models used for iris feature extraction

Representation	FAR (%)	FRR (%)	EER (%)	Database
Hermite	0.0	9.71	2.66	CASIA
Haar [2]	0.0	17.75	2.9	Private
Daubechies 2 [3]	0.001	2.98	0.2687	CASIA
Gabor [15]	0.001	0.12	0.11	NIST (ICE-1)

5 Conclusions and Future Improvements

Results show that the Hermite transform can be used as an alternative method to efficiently characterize iris textures by extracting local information with a pair of Hermite analysis filters. Every stage in an iris recognition system plays a very important role. Since results obtained in previous stages can affect the performance of the system, special attention must be paid in each one. Although the proposed iris recognition system can deal with the iris localization task, some images were less precisely localized than others and as a consequence the CAR decreased. Future localization improvements need to be made in order to decrease the FRR.

References

1. Daugman, J.G.: High confidence visual recognition of persons by a test of statistical independence. IEEE Transactions on Pattern Analysis and Machine Intelligence 15(11), 1148–1161 (1993)
2. Lim, S., Lee, K., Byeon, O., Kim, T.: Efficient iris recognition through improvement of feature vector and classifier. ETRI Journal 23(2), 61–70 (2001)
3. Poursaberi, A., Araabi, B.N.: A half-eye wavelet based method for iris recognition. In: 5th International Conference on Intelligent Systems Design and Applications, pp. 262–267. IEEE Computer Society, Washington (2005)

4. Daugman, J.G.: Uncertainty relation for resolution in space, spatialfrequency, and orientation optimized by two-dimensional visual cortical filters. J. Opt. Soc. Am. A 2(7), 1160–1169 (1985)
5. Bovik, A.C., Clark, M., Geisler, W.S.: Multichannel texture analysis using localized spatial filters. IEEE Transactions on Pattern Analysis and Machine Intelligence 12(1), 55–73 (1990)
6. Clausi, D.A., Ed Jernigan, M.: Designing Gabor filters for optimal texture separability. Pattern Recognition 33(11), 1835–1849 (2000)
7. Martens, J.B.: The Hermite transform-theory. IEEE Transactions on Acoustics, Speech, and Signal Processing 38(9), 1595–1606 (1990)
8. Young, R.A.: Orthogonal basis functions for form vision derived from eigenvector analysis. In: ARVO Abstracts, p. 22. Association for Research in Vision and Ophthalmology, Sarasota (1978)
9. Silvan-Cardenas, J.L., Escalante-Ramirez, B.: The multiscale Hermite transform for local orientation analysis. IEEE Transactions on Image Processing 15(5), 1236–1253 (2006)
10. Rivero-Moreno, C.J., Bres, S.: Texture feature extraction and indexing by Hermite filters. In: 17th International Conference on Pattern Recognition, vol. 1, pp. 684–687. IEEE Computer Society, Washington (2004)
11. CASIAv1.0 Iris Image Database, Chinese Academy of Sciences, Institute of Automation, `http://www.cbsr.ia.ac.cn/IrisDatabase.htm`
12. Canny, F.J.: A computational approach to edge detection. IEEE Transactions on Pattern Analysis and Machine Intelligence 8, 679–698 (1986)
13. Chan, R., Siu, W.C.: A new approach for efficient Hough transform for circles. In: IEEE Pacific Rim Conference on Communications, Computers and Signal Processing, pp. 99–102 (1989)
14. Michaelis, M., Sommer, G.: Basic functions for early vision. Technical Report Bericht 9413, Institut für Informatik und Praktische Mathematik Christian-Albrechts-Universität zu Kiel (August 1994)
15. Daugman, J.G.: New methods in iris recognition. IEEE Transactions on Systems, Man and Cybernetics, Part B 37(5), 1167–1175 (2007)